PNAS
www.pnas.org

Supplementary Information for

Allosteric activation of MALT1 by its ubiquitin-binding Ig3 domain

Rebekka Schairer, Gareth Hall, Ming Zhang, Richard Cowan, Roberta Baravalle, Frederick W. Muskett, Peter J. Coombs, Chido Mpamhanga, Lisa R. Hale, Barbara Saxty, Justyna Iwaszkiewicz, Chantal Décaillet, Mai Perroud, Mark D. Carr, and Margot Thome

Corresponding authors: Margot Thome and Mark D. Carr
Email: *margot.thomemiazza@unil.ch* and *mdc12@leicester.ac.uk*

This PDF file includes:

Supplementary text
Figures S1 to S5
SI References

www.pnas.org/cgi/doi/10.1073/pnas.1912681117

Supplementary Information Text

Materials and Methods

Antibodies

Antibodies used include anti-Tubulin (B-5-1-2), anti-RelB (rabbit polyclonal), anti-phospho-IκBα (Ser32/36) (5A5), anti-IκBα, anti-CARMA1 (CARD11) (1D12) and anti-CYLD (D1A10) from Cell Signaling, anti-BCL10 (331.3, Santa-Cruz), anti-FLAG (M2, Sigma), anti-HA (Covance), anti-JNK1&2 (pTpY183/185) (Biosource) and anti-Roquin-1 (Abcam). The affinity-purified rabbit anti-MALT1 antibody has been previously reported (1). Horseradish peroxidase–coupled goat anti-mouse or anti-rabbit were from Jackson Immunoresearch.

Plasmids

The eYFP-LVSR-eCFP reporter construct and the eukaryotic (pCR3-based) and bacterial (pGEX-based) MALT1 and Ubiquitin constructs have been previously described (2). For CRISPR/Cas9-mediated MALT1 silencing, we used the lentiCRISPRv2 vector from GeCKO. The reconstitution with MALT1 constructs was performed using pWPI vector from Addgene, which allows co-expression of MALT1 and GFP. MALT1 and ubiquitin point mutants were generated by quick-change PCR using Kapa high-fidelity DNA polymerase (Roche) and all mutations were verified by sequencing.

Minimal shift analysis using NMR spectroscopy

Recombinant MALT1 (residues 339-719) with a C-terminal hexahistidine tag was expressed as a soluble product using a pET21a (Novagen) vector transformed into the *E.coli* strain NiCo-21 (NEB). Uniformly $^{13}C/^{15}N$- and ^{15}N- labelled MALT1 were prepared by growing at 37°C in modified Spizizen minimal medium (3) containing $^{15}NH_4SO_4$ (4 g L^{-1}) and/or $^{13}C_6$-glucose (2 g L^{-1}), as required. The protein was purified to homogeneity by chromatography on affinity (Ni-NTA column, Qiagen) and gel filtration (Superdex 75 16/60, GE healthcare) columns, into a final buffer of 20 mM Tris-HCl buffer, pH 7.5, containing 150 mM NaCl and 1 mM TCEP.

Recombinant ubiquitin (residues 1-76) with an N-terminal TEV cleavable hexa-histidine tag was expressed using a pET9a (Novagen) vector transformed into the *E.coli* strain BL-21 (DE3) (NEB). Uniformly ^{15}N- labelled ubiquitin was prepared by growing overnight at 18 °C in modified Spizizen minimal medium (3) containing $^{15}NH_4SO_4$ (4 g L^{-1}). The protein was purified to homogeneity by chromatography on affinity (Ni-NTA column, Qiagen) and gel filtration (Superdex 75 16/60, GE healthcare) columns, into a final buffer of 25 mM HEPES buffer, pH 7.5, 50 mM NaCl and 1 mM TCEP.

All NMR data were acquired on a Bruker Avance III 800 MHz spectrometer equipped with a 5mm HCN cryoprobe. For the ubiquitin binding to MALT1 experiments both the MALT1 (339-

719) at 150 μM and ubiquitin (Sigma, U6253) NMR samples were prepared in 20 mM Tris-HCl buffer, pH 7.5, containing 150 mM NaCl and 1 mM TCEP in 90% H_2O/10% D_2O. The 2D ^{15}N-^{1}H TROSY spectra of MALT1 were obtained at 25°C, in the absence or presence of 0.4 mM, 0.8 mM, 1.2 mM and 1.6 mM ubiquitin. Typical acquisition times for the 2D-NMR experiments were 50 ms in F_2 (^{1}H) and 40 ms in F_1 (^{15}N), with the spectra collected over approximately 4 hours. Backbone amide chemical shifts for free MALT1 were consistent with those reported previously and assigned accordingly (6). All NMR data were processed and analysed using TopSpin and SPARKY (University of California, San Francisco) software. The chemical shift changes in assigned backbone amide signals of MALT1 induced by ubiquitin-binding were used to identify MALT1 residues involved in ubiquitin binding. Backbone amide chemical shift changes were obtained from the combined chemical shift change in ^{15}N and ^{1}H for each assigned peak in the $^{15}N/^{1}H$ TROSY spectrum of the free ^{15}N-labelled MALT1, when compared to the equivalent peak in the $^{15}N/^{1}H$ TROSY spectrum of the ^{15}N-labelled MALT1 sample containing varying concentrations of ubiquitin (4, 5).

The MALT1 E696K/D697K mutant (339-719) at 100 μM and ubiquitin (Sigma, U6253) NMR samples were prepared in 20 mM Tris-HCl buffer, pH 7.5, 150 mM NaCl and 1 mM TCEP, in 90% H_2O/10% D_2O. The 2D $^{15}N/^{1}H$ TROSY spectra of MALT1 E696K/D697K were obtained at 25°C, in the absence or presence of 1.6 mM ubiquitin. Typical acquisition times for the NMR experiments were 50 ms in F_2 (^{1}H) and 40 ms in F_1 (^{15}N).

For the MALT1 addition to ubiquitin experiment, both the ubiquitin (1-76) at 50 μM and MALT1 (339-719) NMR samples were prepared in 25 mM HEPES buffer, pH 7.5, containing 50 mM NaCl and 1 mM TCEP in 90% H_2O/10% D_2O. The 2D ^{15}N-^{1}H TROSY spectra of ubiquitin were obtained at 25°C in the absence or presence of 264 μM MALT1. Typical acquisition times for the double resonance experiments for ubiquitin were 83 ms in F_2 (^{1}H) and 89 ms in F_1 (^{15}N), with the spectra collected over approximately 10 hours. Backbone amide chemical shifts for free ubiquitin were consistent with those reported previously and assignments confirmed with a TOCSY-HSQC spectra. The minimal shift approach was used to identify ubiquitin residues involved in MALT1 binding. Backbone amide minimal shift values were obtained from the combined chemical shift change in ^{15}N and ^{1}H for each assigned peak in the $^{15}N/^{1}H$ TROSY spectrum of the free ^{15}N-labelled ubiquitin, when compared with all peaks observed in the $^{15}N/^{1}H$ TROSY spectrum of the ^{15}N-labelled ubiquitin sample containing 264 μM MALT1.

The ^{15}N-labelled MALT1 Y657A (339-719) NMR sample was prepared in 25 mM HEPES buffer, pH 7.5, containing 50 mM NaCl and 1 mM TCEP in 90% H_2O/10% D_2O. Acquisition times for the $^{15}N/^{1}H$ TROSY experiments were 50 ms in F_2 (^{1}H) and 40 ms in F_1 (^{15}N), with the spectra collected over approximately 4 h. Backbone amide minimal shifts for the MALT1 Y657A mutant were calculated by comparing the $^{15}N/^{1}H$ TROSY spectra from MALT1 Y675A with all peaks observed in the $^{15}N/^{1}H$ TROSY spectrum of the ^{15}N-labelled wild-type MALT1 sample.

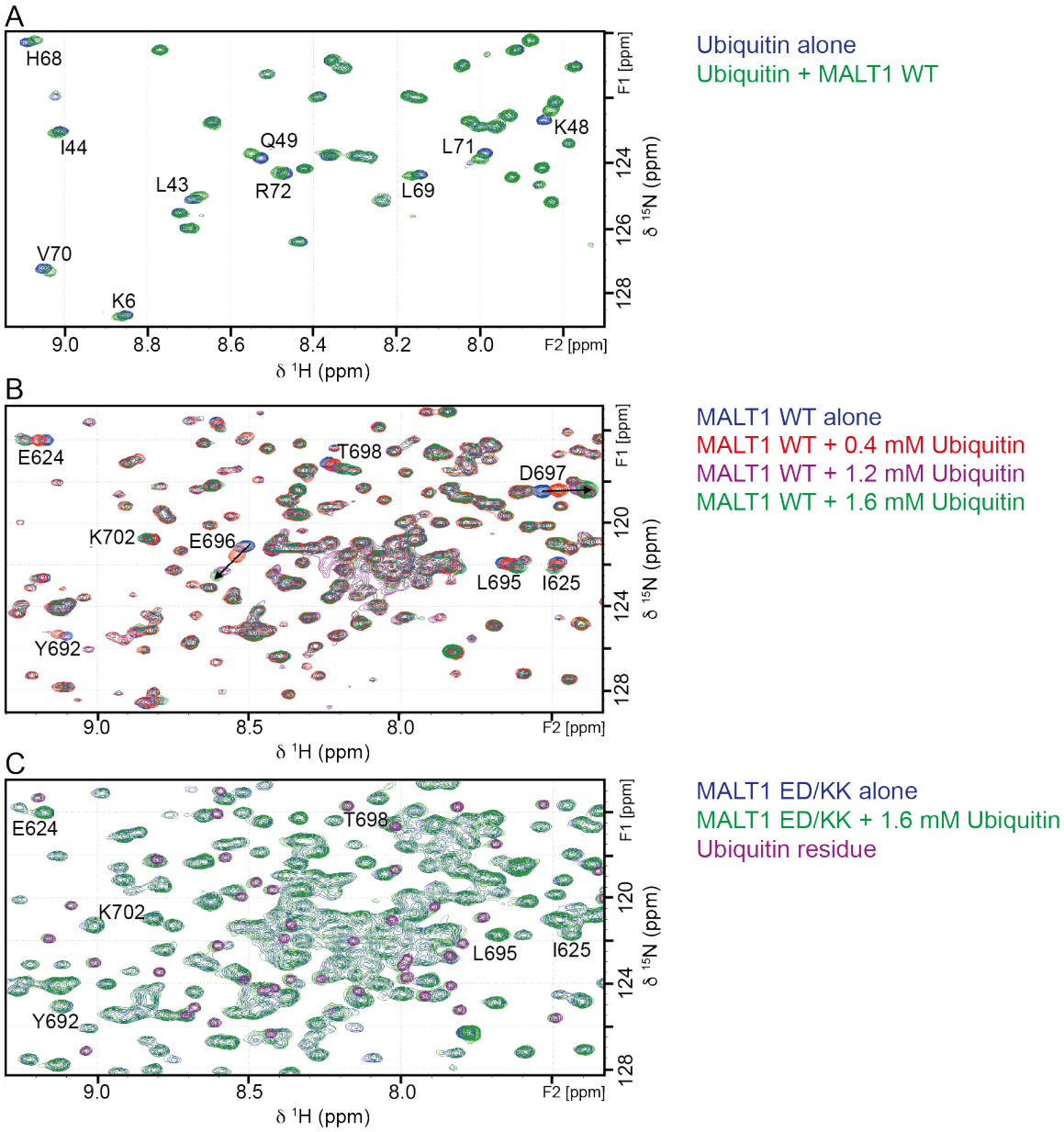

Fig. S1. Ubiquitin interacts with the Ig3 domain *in vitro*. (**A**) A selected region from the ^{15}N-^{1}H TROSY spectra of ^{15}N-labelled ubiquitin alone (blue) and following mixing with MALT1 (green), with the assignments for ubiquitin indicated. It is clear that the backbone amide peaks for K6, L43, I44, K48, Q49, H68, L69, V70, L71 and R72 show reasonable shifts. Images were prepared using Topspin (Bruker Biospin Ltd.). (**B**) A selected region from the ^{15}N-^{1}H TROSY spectra of ^{15}N-labelled MALT1 (0.15 mM) alone (blue) and following the addition of increasing concentrations of human ubiquitin 0.4 mM (red), 0.8 mM (not shown), 1.2 mM (purple) and 1.6 mM (green). The assignments for selected backbone amide signals of MALT1 are indicated. The backbone amide peaks for E696 and D697 show very substantial shifts upon ubiquitin-binding, with significant but somewhat smaller shifts seen for E624, I625, Y692, L695, T698 and K702. (**C**) A selected region from the ^{15}N-^{1}H TROSY spectra of ^{15}N-labelled MALT1 (ED/KK) (0.1 mM) alone (blue) and following the addition of human ubiquitin 1.6 mM (green). Peaks corresponding to natural abundance ^{15}N-ubiquitin are also highlighted (purple). The backbone amide peaks for MALT1(ED/KK) show very little difference following ubiquitin addition.

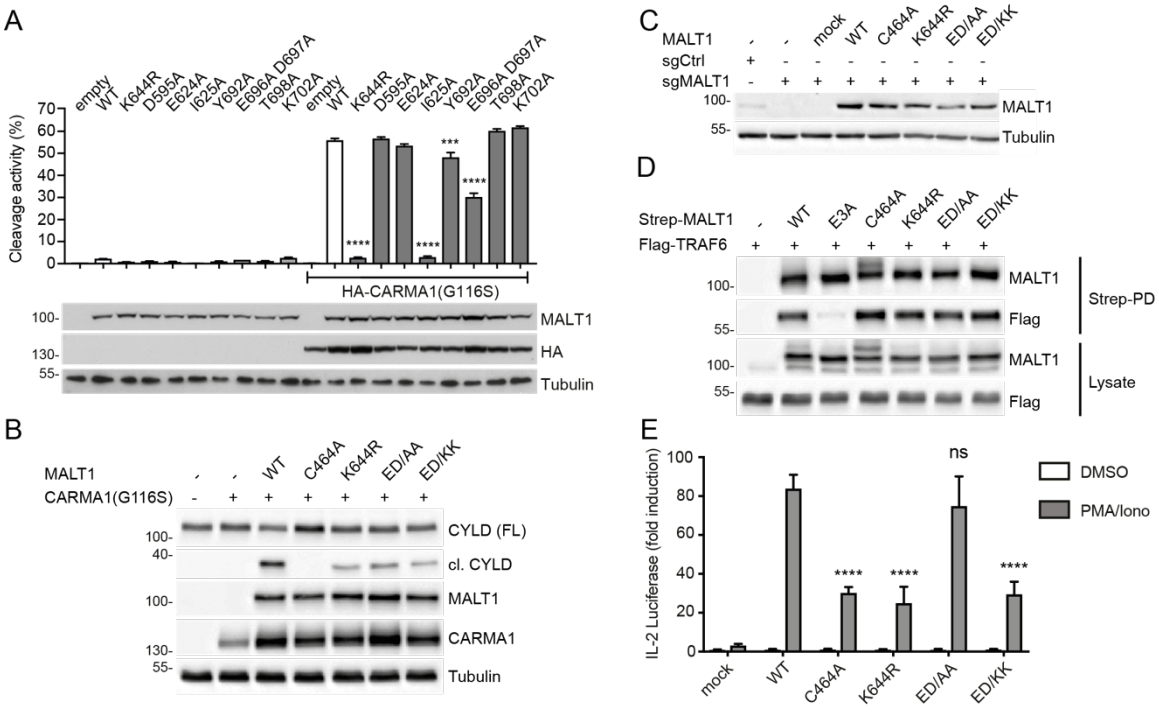

Fig. S2. The Ig3-ubiquitin interaction is necessary for substrate cleavage but dispensable for the scaffold function of MALT1. (**A**) Flow cytometric assessment of MALT1-dependent FRET reporter cleavage in 293T cells. The reporter was co-expressed with the indicated MALT1 constructs and oncogenic CARMA1(G116S). (**B**) 293T cells were transfected with the indicated expression constructs for MALT1, oncogenic CARMA1(G116S) and the MALT1 substrate CYLD and analyzed for substrate cleavage by Western blot as indicated. Positions of full length (FL) and cleaved (cl.) CYLD are indicated. (**C**) Jurkat cells were lentivirally transduced with MALT1-specific or control sgRNAs, as indicated, and MALT1-deficient cells were then transduced with a mock vector or the indicated MALT1 expression constructs. (**D**) 293T cells were transfected with the indicated expression constructs for Strep-tagged MALT1 and Flag-tagged TRAF6, and the capacity of MALT1 to bind to TRAF6 was assessed by Streptactin pull-down (Strep-PD) and Western blot. MALT1 constructs comprise the wild-type (WT) and mutants that are TRAF6 binding-deficient (E3A, mutating E316, E653 and E806 into A), catalytically inactive (C464A), monoubiquitination-deficient (K644R), and mutants of E696 and D697 (ED/AA or ED/KK). (**E**) Luciferase reporter assay of MALT1-deficient Jurkat T cells reconstituted with the indicated constructs of MALT1 and expressing an IL-2 luciferase reporter. Results are presented relative to those of unstimulated cells reconstituted with a mock vector. Positions of molecular weight markers (in kDa) are indicated. Tubulin was used as a loading control (**A, B, C**). Data are representative of two (**A, E**) and three (**B, D**) experiments. Bars represent means ± SD; **P* < 0.05, ***P* < 0.01, ****P* < 0.001, *****P* < 0.0001.

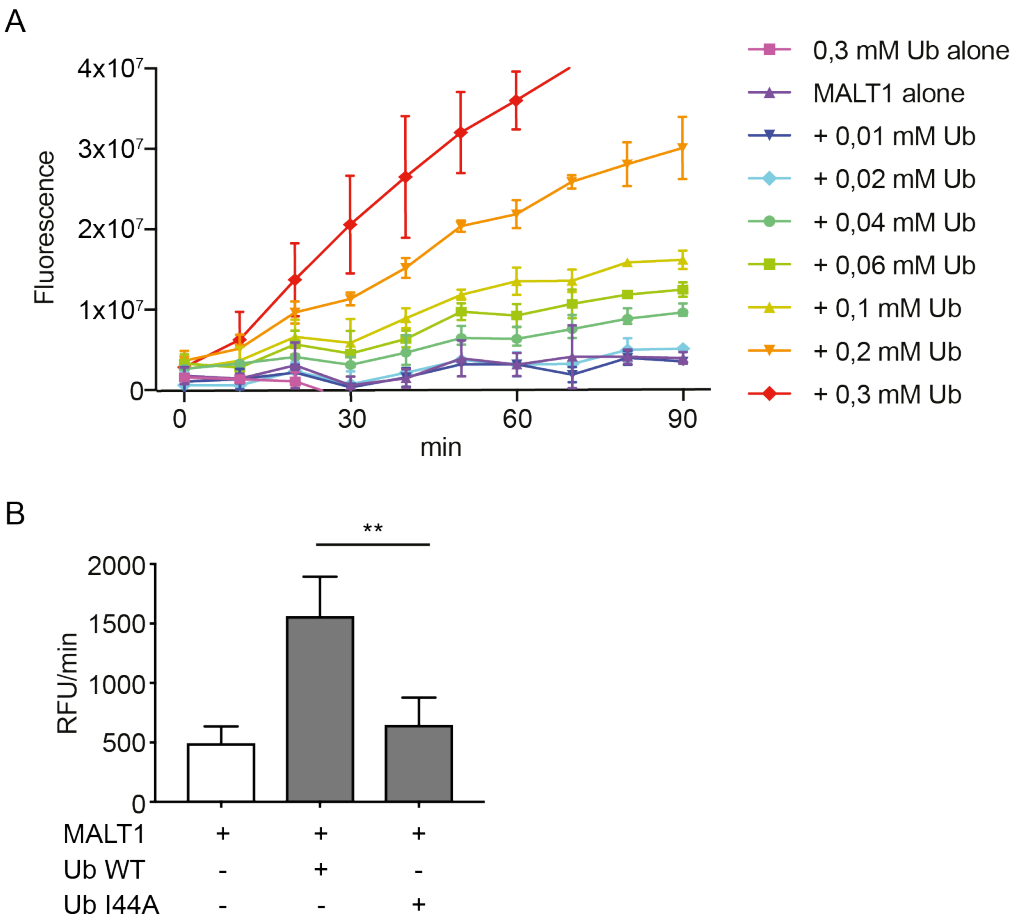

Fig. S3. Monomeric ubiquitin promotes MALT1 protease activity *in vitro*. (**A**) *In vitro* cleavage activity of recombinant purified MALT1 (residues 199-824, 0.6 µM) in presence of the indicated concentrations of recombinant purified ubiquitin. (**B**) *In vitro* cleavage assay comparing the capacity of wild-type ubiquitin and its I44A mutant (both used at 0.1 mM) to activate MALT1.

Data are representative of two (**A**) and three (**B**) experiments. Bars represent means ± SD; $^{**}P < 0.01$.

A

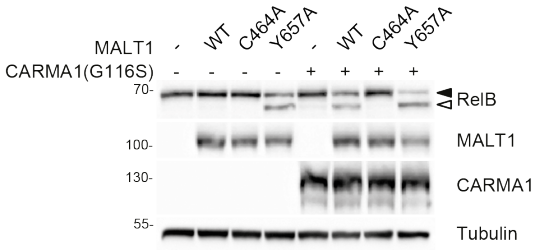
MALT1
CARMA1(G116S)
-
WT
C464A
Y657A
-
WT
C464A
Y657A
-
-
-
-
+
+
+
+
70-
100-
130-
55-
RelB
MALT1
CARMA1
Tubulin

B

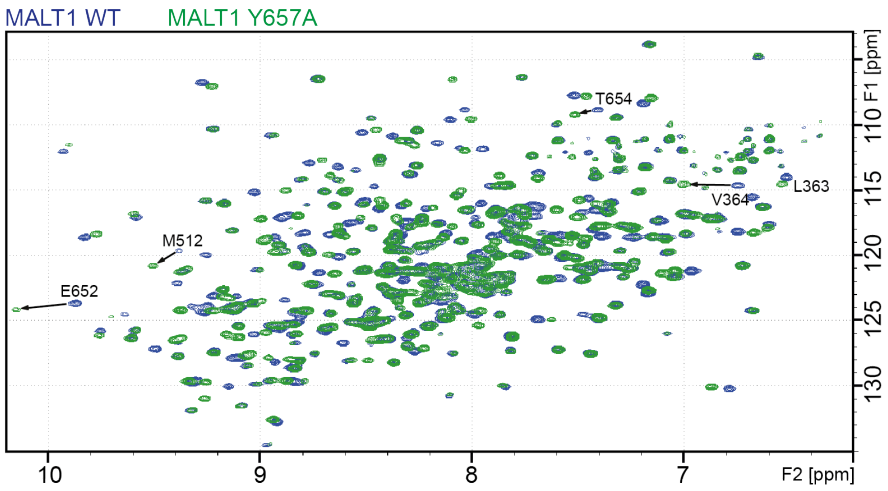
MALT1 WT
MALT1 Y657A
T654
L363
V364
M512
E652
10
9
8
7
F2 [ppm]
110
115
120
125
130
F1 [ppm]

C

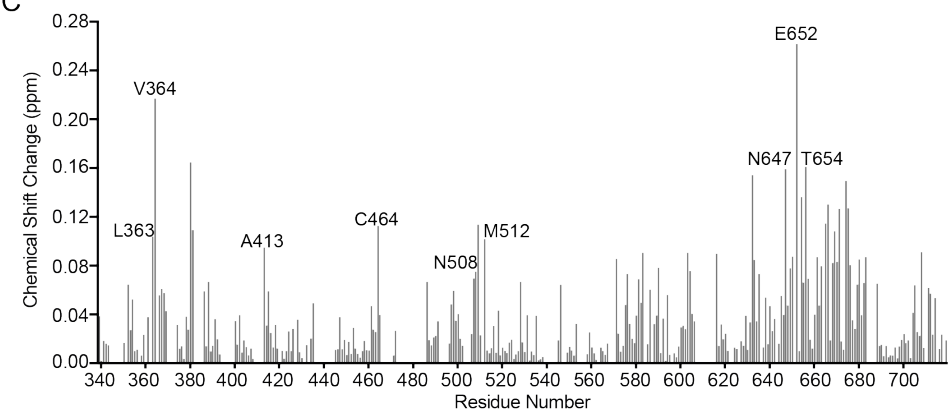
Chemical Shift Change (ppm)
0.28
0.24
0.20
0.16
0.12
0.08
0.04
0.00
E652
V364
N647
T654
L363
A413
C464
M512
N508
340
360
380
400
420
440
460
480
500
520
540
560
580
600
620
640
660
680
700
Residue Number

D

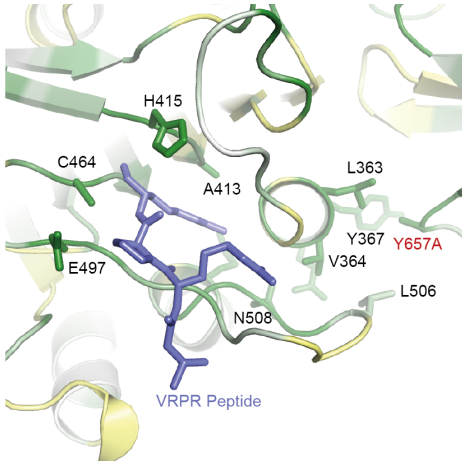
H415
C464
A413
L363
Y367
Y657A
V364
E497
L506
N508
VRPR Peptide

Fig. S4. A hydrophobic cluster of residues around Y657 at the Ig3-protease interface mediates activation of MALT1. (**A**) 293T cells were transfected with the indicated expression constructs for MALT1, oncogenic CARMA1(G116S) and the MALT1 substrate RelB and analyzed for substrate cleavage by Western blot as indicated. Tubulin was used as a loading control. Positions of uncleaved (black arrowhead) and cleaved (open arrowhead) RelB are indicated. The CARMA1-independent RelB cleavage by the Y657A mutation in MALT1 is clearly seen. Data are representative of two experiments. (**B**) A comparison of ^{15}N-^{1}H TROSY spectra obtained for wild-type ^{15}N-labelled MALT1 (residues 339-719, blue) with ^{15}N-labelled MALT1 Y657A (green). Selected residues observed to show very significant shifts in their backbone amide NMR signals are highlighted. (**C**) Histogram revealing the backbone amide minimal shifts seen for ^{15}N-labelled human MALT1 Y675A (residues 339-719) compared to wild-type MALT1. Selected residues observed to show very significant shifts in their backbone amide NMR signals are highlighted. (**D**) Backbone amide chemical shift changes induced by the Y657A mutation in MALT1, mapped onto the reported structure of the Ig3-protease domains. Residues with clearly shifted signals surrounding the active site are highlighted. Residues with significantly perturbed NMR signals (shift > 0.01 ppm) are colored with a gradient from white to green. Residues for which no minimal shift data were obtained are shown in yellow. The expected position of a VRPR substrate peptide bound in the active site of the protease domain is shown as violet sticks. Image was prepared using PyMOL.

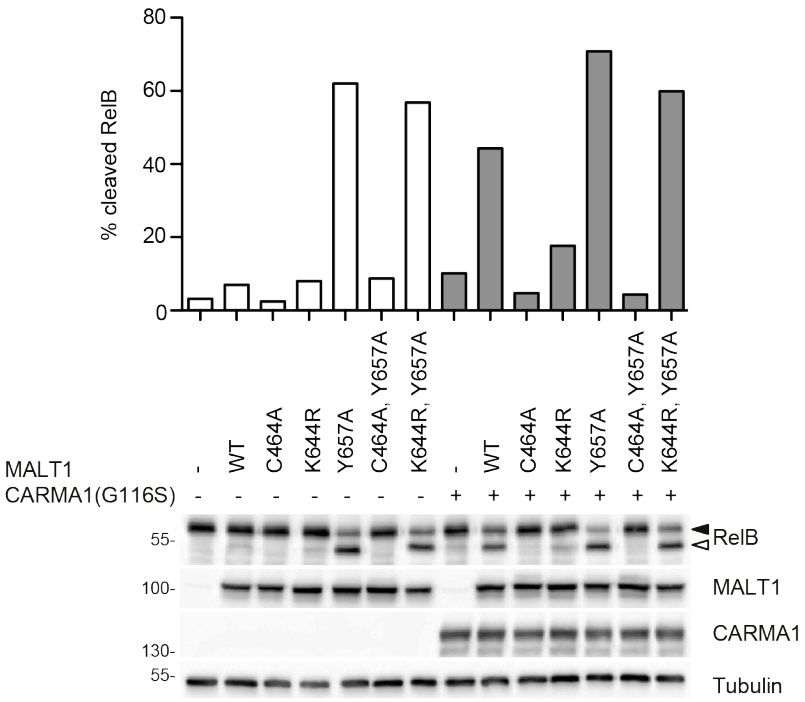

Fig. S5. The MALT1 Y657A mutation overcomes the catalytic defect of the ubiquitination-deficient K644R mutant. 293T cells were transfected with the indicated expression constructs for MALT1, oncogenic CARMA1(G116S) and the MALT1 substrate RelB and analyzed for substrate cleavage by Western blot as indicated. Tubulin was used as a loading control. Positions of uncleaved (black arrowhead) and cleaved (open arrowhead) RelB are indicated. The bar graph shows the quantification of RelB cleavage from the Western blot. Data are representative of a single experiment.

SI References

1. F. Rebeaud *et al.*, The proteolytic activity of the paracaspase MALT1 is key in T cell activation. *Nature Immunol.* **9**, 272-281 (2008).
2. C. Pelzer *et al.*, MALT1 protease activity is controlled by monoubiquitination. *Nature Immunol.* **14**, 337-345 (2013).
3. J. Spizizen, Transformation of Biochemically Deficient Strains of Bacillus Subtilis by Deoxyribonucleate. *Proc Natl Acad Sci U S A* **44**, 1072-1078 (1958).
4. R. A. Williamson, M. D. Carr, T. A. Frenkiel, J. Feeney, R. B. Freedman, Mapping the binding site for matrix metalloproteinase on the N-terminal domain of the tissue inhibitor of metalloproteinases-2 by NMR chemical shift perturbation. *Biochemistry* **36**, 13882-13889 (1997).
5. V. Veverka *et al.*, Structural characterization of the interaction of mTOR with phosphatidic acid and a novel class of inhibitor: compelling evidence for a central role of the FRB domain in small molecule-mediated regulation of mTOR. *Oncogene* **27**, 585-595 (2008).
6. S. Unnerstaale *et al.*, Backbone assignment of the MALT1 paracaspase by solution NMR. *PLoS One* **11**, e0146496 (2016).